Robust Energy Management of Isolated Microgrids

Jose D. Lara, *Member, IEEE*, Daniel E. Olivares, *Member, IEEE*, Claudio A. Cañizares, *Fellow, IEEE*

***Abstract*—This paper presents the mathematical formulation and architecture of a robust Energy Management System for isolated microgrids featuring renewable energy, energy storage and interruptible loads. The proposed strategy addresses the challenges of renewable energy variability and forecast uncertainty using a two-stage decision process combined with a receding horizon approach. The first-stage decision variables are determined using a cutting-plane algorithm to solve a Robust Unit Commitment; the second stage solves the final dispatch commands using a three-phase Optimal Power Flow. This novel approach is tested on a modified CIGRE test system under different conditions. The proposed algorithm is able to produce reliable dispatch commands without considering probabilistic information from the forecasting system. These results are compared with deterministic and stochastic formulations. The benefits of the proposed control are demonstrated by a reduction in load interruption events, and by increasing available reserves without an increase in overall costs.**

***Index Terms*—Microgrid, robust optimization, energy management system, optimal dispatch, Optimal Power Flow, uncertainties.**

NOMENCLATURE

Indices

ω	Non-dispatchable generation units.
g	Dispatchable generation units.
k	Iterations.
kt	Time step for the three-phase OPF.
kt_r	RHOPF simulation time-step counter [5-min].
l	Loads.
n	Number of steps for the look-ahead window
s	ESS units.
S_r	Scenario counter for the simulation.
t	Time step for the RUC.
t_r	RUC simulation time-step counter [1-hr].

Parameters

Γ	Budget of uncertainty [hrs].
${\Delta P_{\omega,t}}^{max}$	Max error, at time t [p.u.].
$\eta_{g_s}^{in}$,$\eta_{g_s}^{out}$	ESS input/output efficiencies for unit s [%].
$\Psi_s^{MP,k}$	Parameter matrix to transfer dual variables to sub-problem.
ρ	Model parameters.
Ξ_s^{MP}	Frontier SoC variables in the OPF from the RUC.
C_g^p	Power cost for g [\$/kW].
C_g^u	Start-up cost for generator g, [\$].
C_g^v	Shut-down cost for generator g, [\$].
C_g^w	Commitment cost for generator g, [\$].
C_c, C_{sh}	Power curtailment and interruptible load cost [\$/kW].
k_{max}	Maximum number of iterations cutting-plane.
M_g^{up}, M_g^{dn}	Min-up and min-down time for unit g [hrs].
P_g^{max}, P_g^{min}	Max and min power limit for unit g [kW].
$P_{\omega,t}^*$	Forecast for unit ω, at time time t [kW].
$P_{l,t}$	Power for load l, at time t [kW].
R_g^{up}, R_g^{dn}	Ramp-up and ramp-down limit for unit g [kW/hr].
$\mathbf{M}$	Constant for the disjunctive constraints.
${\Omega_{\omega,t}}^{SP}$	Parameter to transfer $\Delta P_{\omega,t}$ to the master-problem.
$X^{MP,k}$	Parameters to transfer commitment results to the sub-problem at iteration k.

Sets

$\mathcal{U}$	Uncertainty set.

Variables

$\alpha 1_t^{k+1}$-$\alpha 3_t^{k+1}$, $\alpha 4^{k+1}$	Dual variables of (6a)-(6d).
$\beta 1_t^{k+1}$, $\beta 2_t^{k+1}$	Dual variables of (3b)-(3c).
$\Delta P_{\omega,t}$	Forecast error unit ω, time t, [p.u.].
${\Delta P_{\omega,t}}^+$	Variable for upward error, at time t [p.u.].
${\Delta P_{\omega,t}}^-$	Variable for downward error, at time t [p.u.].
δ	Perturbation in the base RO-problem.
λ_t^{k+1}	Dual variable of (2).
$\mathcal{S}_t$	SoC variables $S_{1,t}$ ... $S_{s,t}$, at time t, [kWh].
$\mu 1_t^{k+1}$, $\mu 2_t^{k+1}$	Dual variables of (3a).
θ	Auxiliary variable.
$\varepsilon 1_{s,t}^{k+1}$-$\varepsilon 6_{s,t}^{k+1}$	Dual variables of (4a)-(4e).
$b1_t^{k+1}$-$b4_t^{k+1}$, $b5^{k+1}$	Disjunctive constraints binary variables.
E_s^{shed}	Energy storage shedding, storage s [kWh].
F_s	Variable to fix $S_{s,t=2}$ to first-stage.
$P_{c,t}$, $P_{s,t}$	Power curtailed and load shed, at time t [kW].
$P_{g,t}$	Power output for unit g, at time t [kW].
$P_{s,t}$	Power output for storage s, at time t [kW].
$P_{s,t}^{out}$, $P_{s,t}^{in}$	ESS output and input power, at time t [kW].
$S_{s,t}$	State-of-Charge of storage unit s, at time t [kWh].
t_u	Time step at which the unit starts or shuts down.
$v_{g,t}$, $u_{g,t}$	Shut-down and start-up for unit g, at time t.
$w_{g,t}$	Status for unit g, at time t.
x_t	Commitment variables vector, $\{w_{g,t}, v_{g,t}, u_{g,t}\}$

This work was supported by Hatch Ltd. through an NRCAN ecoEnergy II Project. The work of D.E. Olivares was supported by the Complex Engineering Systems Institute (CONICYT: FB0816), and SERC-Chile (CONICYT/FONDAP/15110019).

J.D. Lara is with The Energy and Resources Group, University of California Berkeley, Berkeley CA. Email: jdlara@berkeley.edu

D.E Olivares is with the Department of Electrical Engineering and the UC Energy Research Center, Pontificia Universidad Católica de Chile, Santiago, Chile. Email: dolivaresq@ing.puc.cl

C.A. Cañizares is with the Department of Electrical and Computer Engineering, University of Waterloo, Waterloo, ON N2L 3G1, Canada. Email: ccanizares@uwaterloo.ca

I. INTRODUCTION

DRIVEN by sustainability and green energy goals, electrical generation is shifting towards distributed, smaller-scale, non-dispatchable sources based on renewable energy. In

this context, microgrids are key elements in the integration of scattered energy sources, providing control over clusters of local generators and loads [1]. However, there are control challenges associated with a critical demand-supply balance, since renewable energy sources are often low-inertia and averaging effects are limited. These challenges become more apparent in the case of isolated microgrids, due to the lack of real and reactive power support from the main grid [2].

In the literature, these control challenges in isolated microgrids have been tackled using Renewable Energy (RE) forecasts and deterministic Receding Horizon Control (RHC) strategies. Dispatch commands calculated using RHC anticipate the effects of future events such as variations in generation and demand. This approach also accounts for the effects of present actions in future time steps [3]–[7]. However, even though deterministic algorithms based on RHC can handle moderately variable renewable sources, they do not explicitly consider forecasting errors; thus, their performance is strongly dependent on the accuracy of the forecasting engine. Approaches that combine forecasting and dispatch have been proposed to tackle the issue of forecasting uncertainty in the Energy Management System (EMS). A resource-aware utility maximization model for energy management is proposed in [8] which incorporates an Auto-Regressive Moving Average (ARMA) model for RE. Also, an algorithm proposed in [9] is based on Artificial Bee Colony (ABC) to solve the Economic Dispatch (ED) problem, using Artifical Neural Networks (ANN) combined with Markov Chains for online short-term forecasting with error correction; the forecasting model look-ahead window is 7.5 s using data with a 2.5 s data resolution, which is insufficient for Unit Commitment (UC), as it requires longer look-ahead windows. The approach proposed here addresses this shortcoming by incorporating information about the forecasting system's uncertainty into the dispatch algorithm. In this work, historical performance of the forecasting system is used to produce commitment solutions that hedge the microgrid's dispatch against forecasting errors. The EMS is designed using a two-stage decision process, where a novel Robust Unit Commitment (RUC) model is used to decide generators' on/off status, and a detailed three-phase Optimal Power Flow (OPF) is used to determine the actual dispatch of units.

Several recent research papers have proposed uncertainty-aware dispatch strategies. For example, approaches using probabilistic constraints have been implemented in [10]–[12]; however, such probabilistic framework typically requires assumptions regarding the shape of Probability Distribution Functions (PDFs), which may lead to weak representations of uncertainty. In [10], the authors propose a DC-OPF model with probabilistic constraints approximated using scenarios to address computational issues. Another approach presented in [11] considers the RE sources as a disturbance with Gaussian PDF in the nodal power balance equations, approximating the probabilistic constraint using a sample approximation approach. In [12], forecast errors are modeled as independent, normally distributed random variables, which allows rewriting the probabilistic energy-balance equation in an equivalent deterministic form. However, such modeling simplifications do not properly represent the uncertainty of forecasting error, specifically because these do not account for the time-dependency of the random variables and the dynamics of the corresponding probability distributions. In general, these approaches that use a probabilistic framework to account for uncertainty, result in approximated formulations solved with existing optimization models assuming PDFs that may lead to weak representations of uncertainty [13].

As an alternative, scenario-based approaches have been proposed, as for example in [14], where the authors discuss a heuristic methodology that combines a master Stochastic Unit Commitment (SUC) using historical samples with a slave distribution system OPF solved using OpenDSS. However, the use of historical performance scenarios to represent future uncertainty requires abundant data, and does not allow the decision maker to directly adjust the level of conservatism of the models.

In light of the limitations of probabilistic and scenario-based approaches, Robust Optimization (RO) offers an attractive framework for dispatch formulations, accounting for uncertainties without requiring probabilistic assumptions. This characteristic makes RO very appealing for remote microgrid applications, where historical data to generate scenarios might be limited and/or unreliable. For example, a controller proposed in [15] features a distributed robust optimization algorithm for grid-connected microgrids. The solution method requires a central hub that exchanges dual values information with all Distributed Energy Resources (DERs) units, and uses a single polyhedral uncertainty set for all the energy sources in the system. Moreover, this approach is only concerned with the ED problem and does not consider UC or OPF in the formulation. In [16], the authors exploit the decomposable structure of the robust counterpart of a simplified economic dispatch to develop a distributed solution algorithm; the proposed approach guarantees convergence under heterogeneous and asynchronous communications. In [17], the authors present a robust wind dispatch and bidding algorithm with independent uncertainty sets for prices and available generation. The authors in [18] propose a combination of RHC and a robust counterpart to produce safe intervals for the operation of wind power facilities. The work in [19] presents a comprehensive framework for the application of RO in combination with agent-based modeling for a grid-connected microgrid EMS. Uncertainty sets are defined using upper- and lower-limits of random variables without cardinality constraints, which allows the formulation of Mixed-Integer Linear Programming (MILP) robust counterparts.

The recent applications of the RO framework to microgrid EMSs have concentrated on grid-connected microgrids, which feature somewhat different operational challenges. In particular, the issues of critical demand-supply balance and limited system reserves in isolated microgrids make uncertainty management a critical issue in the EMSs for these types of microgrids. Furthermore, EMSs for grid-connected applications feature simplified system models, which are not adequate for isolated microgrids [2]. In view of these limitations, the focus of this paper is the development of an autonomous, automatic dispatch control of generation and loads in isolated microgrids,

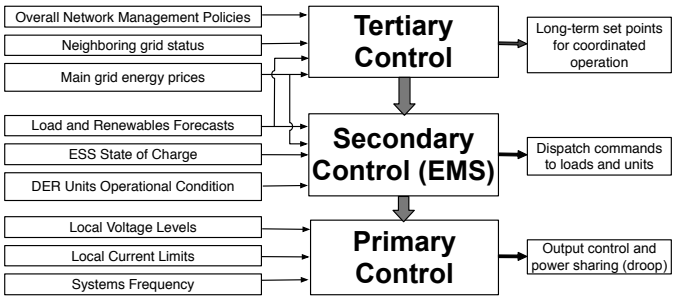

Fig. 1. Hierarchical approach to control of microgrids.

with explicit consideration of the uncertainty associated with forecast values. The present work tackles the aforementioned technical challenges as follows:

- Combine RO and RHC to manage forecasting errors in a novel EMS architecture suitable for the operation of isolated microgrids.
- Use a RUC modeling approach to enable the controller to adjust the reserve levels according to the uncertainty in the RE forecast error.
- A practical and flexible procedure to define polyhedral uncertainty sets based on the past performance of the available forecasting system and the desired level of conservatism.

The resulting dispatch algorithm combines simplified models for the scheduling of units under uncertainty, while retaining a high level of modeling detail for the calculation of final dispatches. The commitment solution of RUC is able to satisfy the constraints for the worst-case scenario in the look-ahead window, given a pre-defined level of conservatism (budget of uncertainty). The final dispatch is refined with a recourse action obtained from a detailed three-phase OPF. The RUC solution results from a primal cutting-plane algorithm based on an uncertainty policy obtained from the analysis of historical forecasting system errors. The second stage OPF is based on the three-phase models in [7], [20] and solved with an interior-point method. The performance of the proposed EMS architecture is compared with a deterministic and a scenario-based Stochastic Optimization (SO)-based approach for different levels of conservatism.

The rest of the paper is structured as follows: Section II presents a background review of relevant dispatch principles to manage uncertainty. Section III provides the details of the proposed architecture to integrate the RO-based UC with a previously proposed three-phase OPF. Section IV describes the proposed RUC formulation for isolated microgrids considering storage, discussing relevant implementation details. Section V presents and discusses simulation results for the proposed robust EMS in a realistic microgrid test system for various case studies. Finally, Section VI highlights some relevant conclusions and the main contributions of the paper.

II. Robust EMS architecture

Figure 1 shows the different control levels, actions and variables associated with each layer of a hierarchical control structure of microgrids, as defined in [2]. Thus, microgrid control tasks are organized hierarchically in 3 layers: primary, secondary, and tertiary controls. The primary control operates at a device level and performs primary regulation using high sampling rates. Secondary controls oversee the operation of the controllable assets within the microgrid, and can operate either in a distributed or centralized fashion, and basically represents the EMS. Tertiary control coordinates the operation of neighboring microgrids. Time frames associated with the tasks in each layer must be properly separated in order to decouple the control actions and prevent interference.

The proposed technique focuses on the secondary control layer, also referred to as the microgrid EMS. The EMS determines appropriate dispatch settings in the microgrid by performing two tasks: a UC and an OPF. In particular, a centralized EMS is assumed to have total control over the DERs. The controller solves the optimal dispatch problem to determine the least-cost power sharing between the assets, considering DER capabilities, reserves, and operational security requirements.

The proposed EMS architecture, depicted in Fig. 2, features a two-stage decision process, combining the solution of a RUC in the first stage, with a highly detailed OPF, proposed in [7], in the second. This is accomplished by using an approximation of the microgrid power dispatch problem as the recourse in the RUC MILP formulation in order to obtain the hedged solution of the first-stage. The RUC sub-problem constitutes a linear approximation of the OPF for the worst-case scenario of $\Delta P_{\omega,t}$, and is used in the master-problem to obtain a hedged commitment solution, as explained in detail in Section IV. Based on the results of the RUC, the three-phase OPF produces the final dispatch decisions. It is important to note that the first decision stage corresponds to a two-stage RO formulation, featuring a linear dispatch model as recourse. Thus, in order to avoid confusion, the second stage of the RUC formulation is referred to as *recourse* hereinafter.

The calculations of the RUC and three-phase OPF use different time resolutions in the forecasting inputs and modeling. This feature enables the use of appropriate forecasting techniques depending on the length of the look-ahead window and required level of detail for each stage. The proposed implementation uses 1-hour time-steps (t) for the RUC, and 5-minute time-steps (k_t) for the three-phase OPF. Also, instead of using constant-length look-ahead windows as in the classical RHC, the proposed EMS has a variable-size three-phase OPF look-ahead window that shrinks in order to keep a fixed boundary condition provided by the RUC. Thus, after the execution of the RUC at a given time-step t, the first OPF is solved at time-step k_t with a look-ahead window that considers 5-minute time-steps $k_t + 1$ to $k_t + 15$, whereas the n^{th} OPF is solved at time-step $k_t + n - 1$, with a look-ahead window that considers 5-minute time-steps $k_t + n$ to $k_t + 15$.

To avoid depleting the available energy from the Energy Storage Systems (ESSs), the OPF requires a target State-of-Charge (SoC) at the end of its shrinking look-ahead window. This target SoC is obtained in the model by defining the SoC of ESSs at the end of the first hour as a first-stage variable in the RUC; thus, a unique target SoC is available for OPF calculations as a frontier condition. The calculation process is shown in Fig. 3 and is summarized as follows:

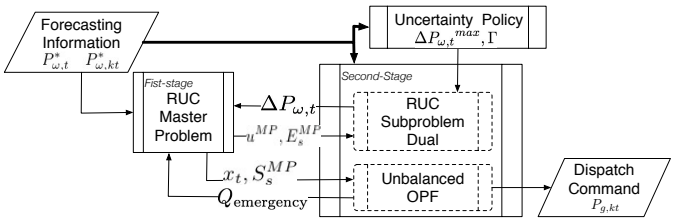

Fig. 2. EMS architecture.

- The RUC is calculated hourly with a 15-minute lead to the corresponding time t, using the most recent forecast generated at the time of execution, where the forecast is updated on an hourly basis. The RUC is solved with a constant length n-hour look-ahead window in order to obtain the commitment decisions and the target SoC of the storage at $t = 2$, which serves as the boundary condition for the three-phase OPF.
- The OPF starts with an initial 75 minute look-ahead window, which corresponds to 15 5-minute k_t steps; this window shrinks as time gets closer to the next hour in order to maintain the same frontier condition (a lower limit of the SoC of ESSs). A new solution of the RUC is calculated when the OPF reaches a 15 minute look-ahead window, providing a new SoC boundary condition and commitment decisions that allows the OPF to reset its look-ahead window to 75 minutes. This 15-minute overlap provides sufficient time for a new run of the RUC, considering corrective actions in case of infeasibility of the OPF. The OPF does not take into account other than the nearest hour, until a new solution of the RUC is available. The forecast used by the OPF has a 5-minute time resolution and is updated every 5 minutes, in order to use the best information available. The final dispatch obtained with a three-phase OPF models is more realistic than the one used in the RUC sub-problem linear model approximation. Also, the frontier condition obtained from the RUC solution allows the OPF to consider future system conditions (beyond the nearest hour) in the operation of ESSs, and prevent the depletion of the ESSs within the OPF horizon.

III. Mathematical Formulation for Robust Microgrid EMS

A. Microgrid Modeling

In order to solve the dispatch problem, the proposed EMS builds on a decomposition approach used in [7], which refines the final calculation using a three-phase OPF. The OPF device models are based on ABCD parameter matrices with phasors represented in rectangular coordinates, proposed in [7], [21]. The following are the main elements of the mathematical formulation of the MILP UC problem:

1) Cost Function: The most common cost function to be minimized is the actual cost of operating the generation units, including fuel and commitment costs. The cost function also includes costs associated with power curtailment and interruptible loads (e.g., demand response), providing complete recourse. It can be represented as follows:

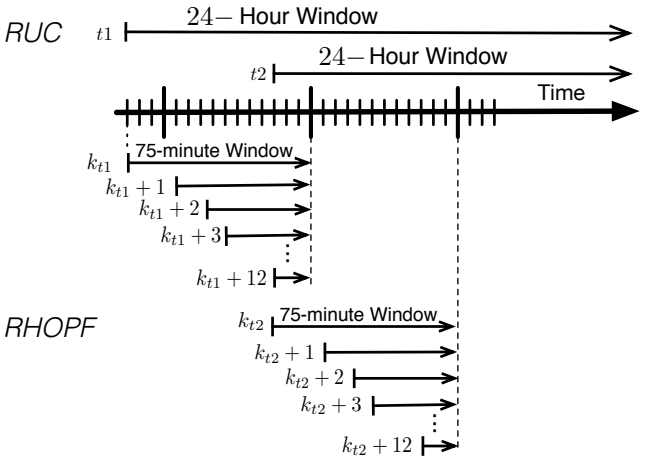

Fig. 3. EMS variable horizons.

$$\sum_t \sum_g \Big[\underbrace{C_g^u u_{g,t} + C_g^v v_{g,t} + C_g^w w_{g,t}}_{\text{Commitment cost}} + \underbrace{C_g^P P_{g,t}}_{\text{Linear fuel cost.}} + \underbrace{C_c P_{c,t}}_{\text{Power curtail cost.}} + \underbrace{C_{il} P_{il,t}}_{\text{Interrupted Load cost.}} \Big] \Delta t \tag{1}$$

2) Operational Constraints: The following constraints ensure supply-demand balance, and guarantee that the the microgrid is operated within acceptable technical limits:

$$\sum_g P_{g,t} + \sum_\omega P^*_{\omega,t}(1 - \Delta P_{\omega,t}) - P_{c,t} = \sum_l P_{l,t} - P_{il,t} \quad \forall t \tag{2}$$

where the uncertainty is represented explicitly by $\Delta P_{\omega,t}$ using an affine parameterization [22]. In principle, this is similar to the reserve value in a deterministic UC.

3) DER Operational Limits: The following DER output and ramping limits must be included, forcing the output to zero if the unit is not committed:

$$P_g^{min} \cdot w_{g,t} \le P_{g,t} \le P_g^{max} \cdot w_{g,t} \qquad \forall t, g \tag{3a}$$
$$P_{g,t} - P_{g,t-1} - u_{g,t} \cdot P_g^{max} \le R_g^{up} \qquad \forall t, g \tag{3b}$$
$$P_{g,t-1} - P_{g,t} - v_{g,t} \cdot P_g^{max} \le R_g^{dn} \qquad \forall t, g \tag{3c}$$

These constraints are of particular importance in microgrid operation with small- and medium-size diesel fleets, in order to avoid carbon build-up [23]. Minimum up and down constraints are also required as follows:

$$u_{g,t} - v_{g,t} = w_{g,t} - w_{g,t+1} \qquad \forall t, g \tag{3d}$$
$$v_{g,t} + u_{g,t} \le 1 \qquad \forall t, g \tag{3e}$$
$$w_{g,t} - w_{g,t-1} - w_{g,t_u} \le 0 \quad \forall t_u : 1 \le t_u - (t-1) \le M_g^{up} \qquad \forall t, g \tag{3f}$$
$$w_{g,t-1} - w_{g,t} + w_{g,t_u} \le 1 \quad \forall t_u : 1 \le t_u - (t-1) \le M_g^{dn} \qquad \forall t, g \tag{3g}$$

Even though DER units in microgrids feature a highly flexible operation, (3d)-(3g) are still necessary in cases where Combined Heat and Power (CHP) units are included or when commitment decisions are revised to account for required reactive power support.

4) ESS Modeling: ESS units s are a subset of the dispatchable units g considered continuously committed, which in addition to the power limits defined by (3a), are subject to other constraints such as the ESS SoC balance constraints and limits, modeled by the following constraints:

$$P_{s,t}^{in} \leq P_s^{max} \qquad \forall t, s \qquad (4a)$$

$$P_{s,t}^{out} \leq P_s^{max} \qquad \forall t, s \qquad (4b)$$

$$P_{s,t} = P_{s,t}^{out} - P_{s,t}^{in} \qquad \forall t, s \qquad (4c)$$

$$S_s^{min} \leq S_{s,t} \leq S_s^{max} \qquad \forall t, s \qquad (4d)$$

$$S_{s,t+1} = S_{s,t} + \left(P_{s,t}^{in} \eta_s^{in} - \frac{P_{s,t}^{out}}{\eta_s^{out}} \right) \Delta t \qquad \forall t, s \qquad (4e)$$

This model can be used to represent a wide range of devices such batteries and hydrogen-storage systems, and is known as the SoC book-keeping model, which is widely used for these types of applications (e.g., [5], [24]).

5) Uncertainty Set Constraints: In order maintain tractability, the uncertainty set must be defined as a simplex, such that the RUC can be modeled as an MILP. In order to accomplish this, polyhedral uncertainty sets $\mathcal{U}$ must be used [25], in which the constraints that represent $\mathcal{U}$ are as follows:

$$\Delta P_{w,t} = \Delta {P_{\omega,t}}^{+} - \Delta P_{w,t}^{-} \qquad \forall t \qquad (5a)$$

$$\Delta {P_{\omega,t}}^{+} - \Delta {P_{\omega,t}}^{max} \leq 0 \qquad \forall t \qquad (5b)$$

$$\Delta {P_{\omega,t}}^{-} - \Delta {P_{\omega,t}}^{max} \leq 0 \qquad \forall t \qquad (5c)$$

$$\sum_t \left[\frac{\Delta {P_{\omega,t}}^{+} + \Delta {P_{\omega,t}}^{-}}{\Delta {P_{\omega,t}}^{max}} \right] - \Gamma \leq 0 \qquad (5d)$$

In the context of this paper, the budget of uncertainty Γ represents the number of periods in which the RE-power deviates from the forecasted value, and $\Delta {P_{\omega,t}}^{max}$ is the maximum value of this mismatch, thus defining a cardinal uncertainty set [26], [27]. This model takes into account the decision-maker risk preference by the selection of Γ and $\Delta {P_{\omega,t}}^{max}$. The parameters of the uncertainty set can be readily obtained from the historical performance of the forecasting system, as discussed next.

B. Robust Optimization UC

The set of equations presented in Section IV-A must be arranged in an RO setting in order to formulate the RUC considering storage. The objective of the RUC model is to yield the least-cost uncertainty-immune solution for the commitment variables given a bounded uncertainty set. The first-stage variables z_{1t}, are calculated before the uncertain variables are revealed. Recourse variables z_{2t}, are determined after the uncertainty is revealed; hence, recourse actions enable the system to adapt to the final outcome of the uncertain variables [28].

In the proposed RUC model for isolated microgrids, the binary variables of the UC problem are determined assuming that the uncertainty is in the forecasted power output of the RE sources only. This problem can be formulated as follows:

$$\min_{z_{1t}} \sum_t^{t+n} J_1(z_{1t}) + \underbrace{\max_{\delta} \min_{z_{2t}} \sum_t^{t+n} J_2(z_{2t}, y_t)}_{\text{Worst-case recourse}} \qquad (6a)$$

$$\text{s.t.} \quad H_1(z_{1t}, \rho) \leq 0 \qquad \forall t \qquad (6b)$$

$$H_2(z_{2t}, y_t, \rho, \mathcal{F}^* | t, \delta) \leq 0 \qquad \forall t \qquad (6c)$$

$$H_3(z_{1t}, z_{2t}, y_t, \rho, \mathcal{F}^* | t, \delta) \leq 0 \qquad \forall t \qquad (6d)$$

$$\delta \in \mathcal{U} \qquad (6e)$$

where J_1 corresponds to the commitment costs in (1) and J_2 represents the other cost terms. Constraints H_1 are deemed part of the first-stage of the RUC, and not affected by $\delta \in \mathcal{U}$. These equations are relevant to first-stage variables $z_{1t} = [w_{1,t} \dots w_{g,t} u_{1,t} \dots u_{g,t} v_{1,t} \dots v_{g,t} S_{1,t=2} \dots S_{s,t=2}]^T$, which in this particular application correspond to equations (3d)-(3g). Also, state variables correspond to the SoCs of ESSs, i.e., $y_t = [S_{1,t} \dots S_{s,t}]^T$ for $t > 2$. Note that in order to maintain $S_{s,t=2}$ as a first-stage variable, the formulation of H_2 does not include $S_{s,t}$ limit constraints (4d), nor the charging equation (4e) for $t = 2$. The system parameters ρ are the different operation limits of the units, such as the ramping rates, maximum and minimum power output, and the ESS efficiencies. Constraints H_2 represents equations (3a)-(3c), (4a)-(4e) for $t > 2$, which are relevant to the recourse variables $z_{2t} = [P_{1,t}, \dots, P_{g,t}, P_{c,t}, P_{sh,t}, P_{1,t}^{out}, \dots, P_{s,t}^{out}, P_{1,t}^{in} \dots P_{s,t}^{in}]^T$. Finally, the uncertainty in the forecast δ, which represents vectors $\delta_\omega = [\Delta P_{\omega,t}, \dots, \Delta P_{\omega,t+n}]$ composed of the individual deviations from the forecast of each non-dispatchable unit ω over the entire look-ahead window. Note that the uncertainty term affects the final solution of the commitment variables, since they are strongly coupled by the system balance constraints (2) and the SoC equations (4d)-(4e) for $t = 2$, which constitute H_3. Thus, the solution takes into account the least favorable realization of the forecasted variable and minimizes the cost of hedging against that particular scenario [29].

C. Nonlinear OPF Model

The OPF model is ESS is similar to the one proposed in [7], representing generators as three-phase sources behind synchronous impedances, transformers and feeders based on ABCD parameter matrices in rectangular coordinates, and loads as a per-phase mix of constant power and constant impedance. The ESS model (4) was also used in [7] to calculate the control and state variables of the ESS; however, given that in the proposed architecture the SoC is a fixed value at the end of the shrinking horizon, a modification is required to avoid expensive load interruption in cases where ESSs are required to charge but the OPF is unable to reach the target SoC. This is achieved by including a positive variable E_s^{shed} in the equation of the frontier condition that is strongly penalized in the objective function, allowing the OPF to lower the

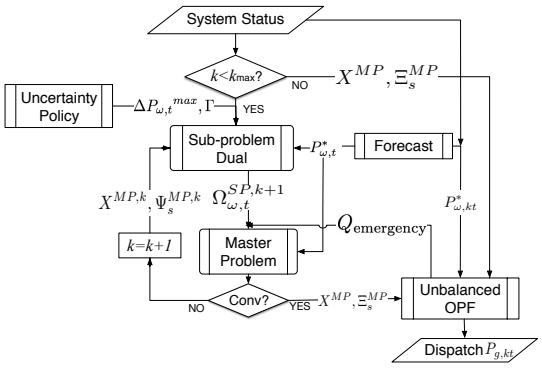

Fig. 4. EMS implementation flow diagram.

target SoC. This can be accomplished by adding the following constraints to the original OPF model:

$$S_{s,k_t+15} = \Xi_s^{MP} - E_s^{shed} \quad \forall s \quad (7a)$$

$$E_s^{shed}\left(\Xi_s^{MP} - S_{s,k_t+n}\right) \geq 0 \quad \forall s \quad (7b)$$

$$E_s^{shed} \leq |S_{s,k_t+n} - \Xi_s^{MP}| \quad \forall s \quad (7c)$$

where S_{s,k_t+n} is a parameter corresponding to the initial SoC in the n^{th} OPF of hour t (initial condition), and S_{s,k_t+15} is a variable corresponding to the SoC at the end of the shrinking horizon (end condition). In this case, the end condition is set equal to the frontier condition from the RUC, i.e., the Ξ_s^{MP} parameter, minus the variable E_s^{shed}. In cases where the RUC sets a target of net charge ($S_{s,k_t+n} < \Xi_s^{MP}$), equation (7c) limits variable E_s^{shed} to a maximum of $\Xi_s^{MP} - S_{s,k_t+n}$, whereas equation (7b) forces E_s^{shed} to zero for target of net discharge.

IV. Robust Dispatch Implementation

The proposed EMS implementation solves the RUC first using the primal cutting-plane decomposition algorithm which employs a master- and sub-problem iterative framework [30], [31].The primal cutting-plane algorithm is regarded as a constraint-and-column generation strategy or delayed column generation [32].

The proposed implementation is shown in Fig. 4, the master-problem determines the commitment ($x_t^{k+1} = [u_{g,t}^{k+1}, v_{g,t}^{k+1}, w_{g,t}^{k+1}]$) and frontier condition of the ESSs SoC ($\mathcal{S}_{t=2}^{k+1}$) for a given $\Delta P_{\omega,t}{}^{k}$. The sub-problem determines $\Delta P_{\omega,t}{}^{k+1}$ using a solution from the commitment x_t^k and $\mathcal{S}_{t=2}^k$ from the previous iteration. The result is used to build the cuts introduced in the master-problem at each k-iteration. The method iterates exchanging the information about the cuts and the commitment decisions, until the RUC solution is obtained either by achieving convergence or reaching the maximum iteration k_{max}. Finally, based on the RUC solutions $X^{MP,k}$ and Ξ_s^{MP}, and using the three-phase OPF models proposed in [7], the controller calculates the final dispatch. In order to avoid infeasibility of the OPF due to reactive power shortage, the formulation considers additional sources of reactive power that can provide unlimited reactive power support at a very high cost; the total reactive power injection from all these sources is denoted as $Q_{emergency}$. In cases where the solution of the OPF yields a non-zero $Q_{emergency}$, the RUC is required to bring on-line more units than the previous solution of the RUC [7].

A. Master Problem

The master-problem is defined as follows:

$$\min_{x_{g,t}^{k+1}, P_{g,t}^{k+1}} \sum_t \sum_g \left[C_g^u u_{g,t}^{k+1} + C_g^v v_{g,t}^{k+1} + C_g^w w_{g,t}^{k+1}\right] + \theta \quad (8a)$$

s.t.

$$\sum_t \left[C_{sh} P_{sh,t}^{k+1} + C_c P_{c,t}^{k+1} + \sum_g C_g P_{g,t}^{k+1}\right] \leq \theta \; \forall k \quad (8b)$$

$$S_{s,t=2}^{k+1} = F_s \quad \forall k, s \quad (8c)$$

$$H_1\left(x_t^{k+1}\right) \leq 0 \quad \forall t \quad (8d)$$

$$H_2\left(x_t^{k+1}, P_{g,t}{}^{k+1}, \mathcal{S}_t^{k+1}, \Omega_{\omega,t}{}^{SP,k+1}\right) \leq 0 \quad \forall k,\ t \quad (8e)$$

where θ separates the objective function (1) into the terms affected by uncertainty and the ones that are not, i.e., upper- and lower-level problems respectively. The RUC solution algorithm introduces a finite set of constraints primal to the first stage (i.e., (8b)-(8c) and (8e)) at each iteration from the solution of the sub-problem. The vector functions H_2 represents these system constraints, which are introduced as cuts at each iteration k. and the vector function H_1 corresponds to the constraints relevant only to the master-problem and not included in the cuts. Constraint (8c) forces $S_{s,t=2}^k$ as first-stage variables by fixing them for each iteration to the variable F_s; this activates all the cuts relevant to $S_{s,t=2}$ at each iteration.

B. Sub-problem

The sub-problem is used to generate the least favorable $\Delta P_{\omega,t}{}^{k+1}$, given the solution $X^{MP,k}$ and $\mathcal{S}_{t=2}^k$ from the master-problem at each iteration, until convergence is attained. This mathematical problem can be defined as follows:

$$\max_{\Delta P_{\omega,t}{}^{k+1}} \min_{P_{g,t}{}^{k+1}} \sum_t \left[C_{sh} P_{sh,t}^{k+1} + C_c P_{c,t}^{k+1} + \sum_g C_g^P P_{g,t}^{k+1}\right] \quad (9a)$$

$$\text{s.t.} \quad H_2'\left(X^{MP,k}, \mathcal{S}_{t=2}^k, \mathcal{S}_t'^{k+1}, P_{g,t}^{k+1}, \Delta P_{\omega,t}^{k+1}\right) \leq 0 \; \forall t \quad (9b)$$

$$\delta_\omega^{k+1} \in \mathcal{U} \quad \forall t \quad (9c)$$

Note that the sub-problem does not optimize variable $S_{s,t=2}$, corresponding to equations (4d) and (4e) for $t = 2$. Thus, $\mathcal{S}'$ and H_2' are subsets of $\mathcal{S}$ and H_2, corresponding to $\mathcal{S}$ and H_2 without $S_{s,t=2}$ and its constraints. The resulting sub-problem has a max-min structure, which can be transformed into a max-max formulation by using the dual of the dispatch variables, this dualization introduces bi-linear terms as reported in the RUC literature (e.g., [28]); however, these terms can be eliminated transforming the problem using the KKT conditions [33]. The resulting model is an MILP problem, obtained using disjunctive constraints [34]. Also, since H_2' does not include variables $S_{s,t=2}$, the missing dual variables needed to solve the sub-problem are obtained from the master-problem, as shown in (10f), where the dual variables are equated to

the master-problem duals from the previous iteration. The resulting MILP model is as follows:

$$\max_{\substack{\lambda^{k+1},\mu^{k+1},\\ \varepsilon^{k+1},\alpha^{k+1},\\ \beta^{k+1},\\ {\Delta P_{\omega,t}}^{max\,k+1}}} \sum_t \Bigg[\lambda_t^{k+1}\Big[\sum_l P_{l,t} - \sum_\omega P^*_{\omega,t}\Big] + \Big[{\Delta P_{\omega,t}}^{max}(\alpha 2_{\omega,t}^{k+1} + \alpha 3_{\omega,t}^{k+1})\Big] + \Gamma\alpha 4_\omega^{k+1} + \sum_g \Big[\mu 1_{g,t}^{k+1} P_g^{max} w_{g,t}^k - \mu 2_{g,t}^{k+1} P_g^{min} w_{g,t}^k + \beta 1_{g,t}^{k+1}(R_g^{up} + u_{g,t}^k P_g^{max}) + \beta 2_{g,t}^{k+1}(R_g^{dn} + v_{g,t}^k P_g^{max})\Big] + \sum_s \Big[\mu 1_{s,t}^{k+1} P_s^{max} w_{s,t}^k - \mu 2_{s,t}^{k+1} P_s^{min} w_{s,t}^k + \varepsilon 2_{s,t}^{k+1} S_s^{max} - \varepsilon 3_{s,t}^{k+1} S_s^{min} - \varepsilon 5_{s,t}^{k+1} P_s^{max} + \varepsilon 6_{s,t}^{k+1} P_s^{max}\Big]\Bigg] \quad (10a)$$

s.t.

$$\lambda_t^{k+1} + \mu 1_{g,t}^{k+1} - \mu 2_{g,t}^{k+1} + \beta 1_{g,t}^{k+1} - \beta 1_{g,t-1}^{k+1} - \beta 2_{g,t}^{k+1} + \beta 2_{g,t-1}^{k+1} \le C_g^P \quad \forall t, g \quad (10b)$$

$$\lambda_t^{k+1} + \mu 1_{s,t}^{k+1} - \mu 2_{s,t}^{k+1} + \beta 1_{s,t}^{k+1} - \beta 1_{s,t-1}^{k+1} - \beta 2_{s,t}^{k+1} + \beta 2_{s,t-1}^{k+1} + \varepsilon 1_{s,t}^{k+1} \le 0 \quad \forall t, s \quad (10c)$$

$$\lambda_t^{k+1} \le C_{sh} \quad \forall t \quad (10d)$$

$$\lambda_t^{k+1} \le C_c \quad \forall t \quad (10e)$$

$$[\varepsilon 2_{s,t+1}^{k+1} \quad \varepsilon 3_{s,t+1}^{k+1} \quad \varepsilon 4_{s,t+1}^{k+1}] = \Psi_s^{MP,k} \quad \forall s \quad (10f)$$

$$\varepsilon 2_{s,t}^{k+1} - \varepsilon 3_{s,t}^{k+1} - \varepsilon 4_{s,t}^{k+1} + \varepsilon 4_{s,t-1}^{k+1} \le 0 \quad \forall t, s \quad (10g)$$

$$-\varepsilon 1_{s,t}^{k+1} + \varepsilon 4_{s,t}^{k+1} \frac{1}{\eta_s^{out}} \Delta t \le 0 \quad \forall t, s \quad (10h)$$

$$\varepsilon 1_{s,t}^{k+1} - \varepsilon 4_{s,t}^{k+1} \eta_s^{in} \Delta t \le 0 \quad \forall t, s \quad (10i)$$

$$\alpha 1_t^{k+1} = \lambda_t^{k+1} \sum_\omega P^*_{\omega,t} \quad \forall t \quad (10j)$$

$$\Delta P_{\omega,t}^{k+1} = {\Delta P_{\omega,t}^+}^{k+1} - {\Delta P_{\omega,t}^-}^{k+1} \quad \forall t \quad (10k)$$

$$0 \le \alpha 2_t^{k+1} \le \mathbf{M}(1 - b1_t^{k+1}) \quad \forall t \quad (10l)$$

$$0 \le -{\Delta P_{\omega,t}^+}^{k+1} + {\Delta P_{\omega,t}}^{max} \le \mathbf{M} b1_t^{k+1} \quad \forall t \quad (10m)$$

$$0 \le \alpha 3_t^{k+1} \le \mathbf{M}(1 - b2_t^{k+1}) \quad \forall t \quad (10n)$$

$$0 \le -{\Delta P_{\omega,t}^-}^{k+1} + {\Delta P_{\omega,t}}^{max} \le \mathbf{M} b2_t^{k+1} \quad \forall t \quad (10o)$$

$$0 \le {\Delta P_{\omega,t}^-}^{k+1} \le \mathbf{M}(1 - b3_t^{k+1}) \quad \forall t \quad (10p)$$

$$0 \le \alpha 1_t^{k+1} + \alpha 3_t^{k+1} + \frac{\alpha 4^{k+1}}{{\Delta P_{w,t}}^{max}} \le \mathbf{M} b3_t^{k+1} \quad \forall t \quad (10q)$$

$$0 \le {\Delta P_{\omega,t}^+}^{k+1} \le \mathbf{M}(1 - b4_t^{k+1}) \quad \forall t \quad (10r)$$

$$0 \le -\alpha 1_t^{k+1} + \alpha 2_t^{k+1} + \frac{\alpha 4^{k+1}}{{\Delta P_{w,t}}^{max}} \le \mathbf{M} b4_t^{k+1} \quad \forall t \quad (10s)$$

$$0 \le \alpha 4^{k+1} \le \mathbf{M}(1 - b5^{k+1}) \quad (10t)$$

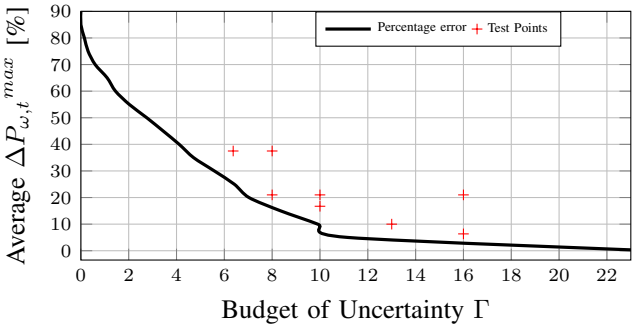

Fig. 5. Cumulative characteristics of the data error from [6].

$$0 \le -\sum_t \left[\frac{{\Delta P_{\omega,t}^+}^{k+1} + {\Delta P_{\omega,t}^-}^{k+1}}{{\Delta P_{\omega,t}}^{max}}\right] + \Gamma \le \mathbf{M} b5^{k+1} \quad (10u)$$

C. Uncertainty policy

The parameters ${\Delta P_{\omega,t}}^{max}$ and Γ define the uncertainty policy, and reflect the decision-maker's preferences on the level of hedging. It is proposed here that Γ be obtained by an analysis of the forecasting errors based on the error duration curve. For the example depicted in Fig. 5, using the forecasting data from [6], the curve shows that as ${\Delta P_{\omega,t}}^{max}$ increases, the number of periods Γ decreases, thus, the selection must be coherent with this behavior. Also, since the duration curve represents the average error characteristics, the value of the parameters should be on the right-hand side of the curve in order to be more conservative than average, as shown by the $+$ symbols in Fig. 5, for this particular set of data. Another relevant information that must be selected by the decision-maker is ${\Delta P_{\omega,t}}^{max}$, depending on the forecast look-ahead time t. These bounds can be obtained from an appropriate forecasting system or by previous performance analysis.

The models are coded in the high-level optimization modeling language GAMS [35]. The simulations were executed using the graphical user interface of GAMS, where the RUC (MILP) and the three-phase OPF (Nonlinear Programming (NLP)) were solved using CPLEX 12.1 [36] and COIN-IPOPT 3.7 solvers [37], respectively. All the simulations were performed in a computer featuring an Intel Xeon CPU L7555 at 1.86 GHz (4 processors), and 64 GB of RAM. The EMS is assumed to have full control and information of every DER in the microgrid.

V. Results

The designed robust EMS is tested on a modified version of the medium-voltage grid-connected microgrid in [38], replacing what was originally a connection to the main grid with two main diesel generation units [20]. This configuration is typical of isolated microgrids, where diesel generators are connected to the medium-voltage network through a step-up transformer [23]. The system has been used and extensively documented for EMS testing in [7] and [20]. The details regarding system parameters and configuration are provided in the Appendix of [7]. The system features 2 diesel units

with capacities of 1750 kW and 800 kW, and a smaller diesel of 310 kW as a distributed resource. The system's total installed capacity is 6,400 kW, including ESS units, controllable and intermittent DERs. The microgrid's load is unbalanced, with a peak of 4,340 kW. The proposed EMS is tested using eight combinations of uncertainty policy, defined by the pair $(\Gamma, \Delta P_{\omega,t}^{max})$ (see Fig. 5) and compared with a deterministic formulation that does not consider uncertainty in the forecast. This test was carried out substituting the proposed RUC formulation with a deterministic UC, and maintaining the same RHC structure.

A. Experimental set-up

In order to test the performance of the EMS, two different simulation experiments were carried out. Experiment 1 uses an actual 24-hour wind power realization with 5-min resolution obtained from an isolated microgrid in Huatacondo, Chile [6], where for each uncertainty policy, 24 hours of operation were simulated to characterize the performance of the EMS in terms of cost, reserves, and SoC. Specifically, at each hour of operation, the UC is calculated by the RUC module of the EMS, and then the dispatch is calculated every 5 minutes by the OPF module as described in Section II.

Experiment 2 consists of several 24-hour simulations performed using a set of synthetic scenarios to test the robustness of the proposed approach for several possible realizations of wind power. Twenty profiles were generated using the technique described in [39], and the results of the simulations were compared based on two performance metrics: total cost, and daily average spinning reserve. The actual realization, a 24-hour forecast and the twenty generated scenarios are depicted in Fig. 6.

The implementation of the process is shown in Fig. 7, where three loops are shown. The outer loop corresponds to the execution of the EMS 24-hour cycle for each scenario indexed by S_r. For each scenario, two inner loops are used to simulate the EMS operation replicating the process described in Fig. 3. The first inner loop corresponds to the RUC that runs every hour, indexed by t_r. The second inner loop corresponds to the 15 OPF calculation steps with variable lengths, using the solution from the RUC, and indexed using kt_r. All the simulations are based on the same 24-hour forecast for the RUC, in order to study the impact of deviations with a higher time resolution.

1) Experiment 1: The simulations shows that given the low cost of the microturbine, and the size of $G3$ (1,750 kW diesel unit), these provide the base load. The scheduling of diesel units $G1$ (800 kW) and $G2$ (310 kW), is shown in Table I. These diesel units are of particular interest in the analysis, since they provide reserves for the operation of the microgrid; hence, their scheduling adapts to the uncertainty considerations.

The system's average reserve levels for different uncertainty policies, corresponding to the available power from thermal units, are between 75% and 100% higher. The levels of reserve increase as the level of conservatism of the UCs increases, i.e., $(\Gamma, \Delta P_{\omega,t}^{max})$, yielding more secure system conditions against variations on the availability of RE resources. The most relevant difference is between hours 12-24, where the RUC formulation commits more capacity than the deterministic case, as shown in Table I.

TABLE I
UC RESULTS

Case		Hours																							
	g	1	2	3	4	5	6	7	8	9	10	11	12	13	14	15	16	17	18	19	20	21	22	23	24
Deterministic	G1	0	0	0	0	0	0	1	1	1	1	1	0	0	0	0	0	0	0	0	0	0	0	0	0
	G2	0	0	0	0	0	1	1	1	1	1	1	1	1	1	1	1	0	0	0	0	0	0	0	0
RO-Based (Γ=6.3, ΔP=37%)	G1	0	0	0	0	0	0	1	1	1	1	1	1	1	1	1	1	0	0	0	0	0	0	0	0
	G2	0	0	0	0	0	1	1	1	1	0	0	0	0	0	0	0	1	1	1	1	1	1	1	1
RO-Based (Γ=8, ΔP=21%)	G1	0	0	0	0	0	0	1	1	1	1	1	0	0	1	1	1	0	0	0	0	0	0	0	0
	G2	0	0	0	0	0	1	1	1	1	1	1	1	1	0	0	1	1	1	1	1	1	1	1	0
RO-Based (Γ=8, ΔP=37%)	G1	0	0	0	0	0	0	1	1	1	1	1	0	0	1	1	1	0	0	0	0	0	0	0	0
	G2	0	0	0	0	0	1	1	1	1	0	0	0	0	0	0	0	1	1	1	1	1	1	1	0
RO-Based (Γ=10, ΔP=21%)	G1	0	0	0	0	0	0	1	1	1	1	1	0	0	1	1	1	0	0	0	0	0	0	0	0
	G2	0	0	0	0	0	1	1	1	1	0	0	0	0	0	0	0	1	1	1	1	1	1	1	1
RO-Based (Γ=13, ΔP=10%)	G1	0	0	0	0	0	0	1	1	1	1	1	0	1	1	0	0	0	0	0	0	0	0	0	0
	G2	0	0	0	0	0	1	1	1	1	1	1	1	1	1	1	1	1	1	1	1	1	1	1	0
RO-Based (Γ=16, ΔP=21%)	G1	0	0	0	0	0	0	1	1	1	1	1	0	0	1	1	1	0	0	0	0	0	0	0	0
	G2	0	0	0	0	0	1	1	1	1	1	1	1	1	0	0	1	1	1	1	1	1	1	1	1
RO-Based (Γ=16, ΔP=6.3%)	G1	0	0	0	0	0	0	1	1	1	1	1	0	0	0	0	0	0	0	0	0	0	0	0	0
	G2	0	0	0	0	0	1	1	1	1	1	1	1	1	1	1	1	1	1	1	1	1	1	1	0

Considering that the average level of reserve is not the only measure of interest, the instantaneous level of reserve and the SoC of the ESS during the 24-hour simulation are shown in Figs. 8 and 9 respectively. Note that the RUC provides more reserves to the system as compared with the deterministic case for all the variants of the uncertainty policy.

TABLE II
COST COMPARISON BETWEEN UNCERTAINTY POLICY.

Case	Fuel Cost [1000$]	Interruptible Load Cost [1000$]	Total Cost [1000$]
Deterministic	12.69	1.20	15.70
(Γ=6.3,$\Delta P_{\omega,t}^{max}$=37%)	12.66	0.88	14.85
(Γ=8,$\Delta P_{\omega,t}^{max}$=21%)	12.72	0.50	13.98
(Γ=8,$\Delta P_{\omega,t}^{max}$=37%)	12.47	0.92	14.76
(Γ=10,$\Delta P_{\omega,t}^{max}$=21%)	12.56	0.47	13.74
(Γ=10,$\Delta P_{\omega,t}^{max}$=16.72%)	12.67	0.92	14.96
(Γ=13,$\Delta P_{\omega,t}^{max}$=10%)	12.69	0.60	14.18
(Γ=16,$\Delta P_{\omega,t}^{max}$=21%)	12.46	0.35	13.33
(Γ=16,$\Delta P_{\omega,t}^{max}$=6.33%)	12.81	0.57	14.22

There is a significant reduction of total cost of interruptible load depending on the selected uncertainty policy without a significant increase in fuel costs (see Table II), yielding lower total costs of operation. The reduction ranges between 28% and 70%, with the best results being obtained for the policy (16, 21%), as shown in Fig. 6.

2) Experiment 2: The frequency plots for the simulation of the RO-based EMS results of the 20 synthetic wind profiles are depicted in Figs. 10-12. In addition to a comparison of the uncertainty policies with the deterministic approach, the RUC is also compared here with respect to a state-of-the-art SO-based EMS proposed in [20]. Figure 10 shows fuel cost reductions in most cases for the RO-based approach for various uncertainty policies when compared with the deterministic and stochastic methods. This is due to the fact that proposed EMS dispatches more power from the ESSs during peak hours to compensate for potential variations of wind power,

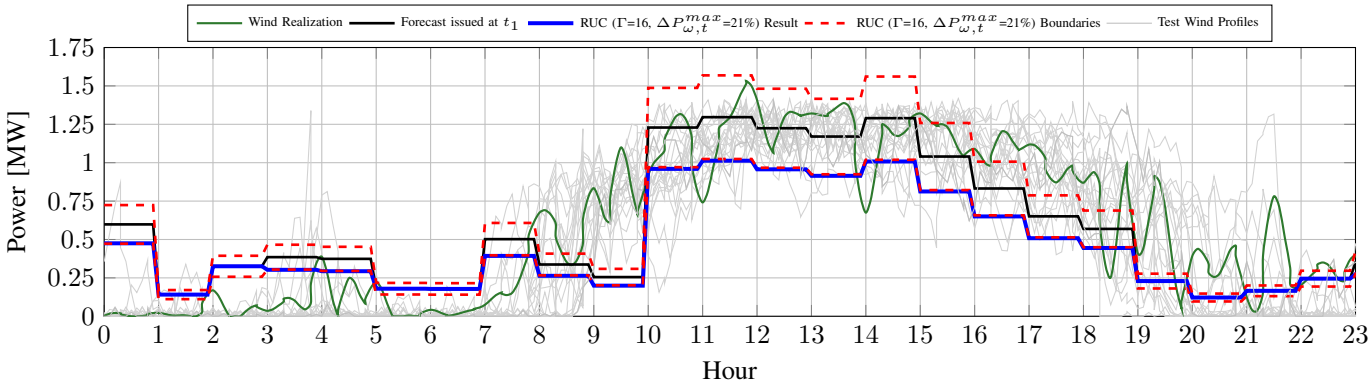

Fig. 6. RUC results for uncertainty policy (16,21%) and wind realization scenarios and forecast at t_1.

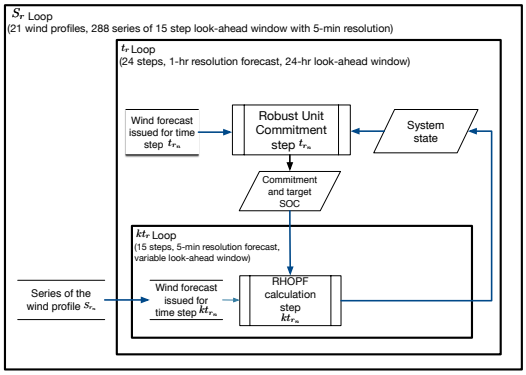

Fig. 7. Experimental set-up of the scenario simulations.

TABLE III
ITERATION COUNT OF THE RUC ALGORITHM FOR DIFFERENT UNCERTAINTY POLICIES.

Γ	$\Delta P_{\omega,t}^{max}$	Min iteration	Max iteration
6.37	37.5	1	4
8	37.5	1	3
10	16.72	1	3
16	6.335	1	3
8	21	1	4
13	10	1	3
16	21	1	3
10	21	1	4
10	37	No convergence after 10 iterations	
16	30	No convergence after 10 iterations	
16	37	No convergence after 10 iterations	

as illustrated in Fig. 9. Figure 11 shows the effectiveness of the proposed EMS technique to reduce the total cost of operation, including fuel and interruptible loads in a resource constrained system. Note the higher fuel cost incurred by the SUC approach, which yields slightly lower total costs due to less use of interruptible loads. Nevertheless, the total costs obtained by the RO-based dispatch are quite stable for different calibrations of the uncertainty set. This is an advantage of the proposed approach with respect to the SO-based dispatch, whose performance strongly depends on the quality of the generated scenarios [20].

From the reserves perspective, the combined results of Figs. 8 and 12 show that, in general, the use of RUC is able to allocate more reserves at times of higher RE penetration than the deterministic approach, in order to keep the system secure; furthermore, the RO-based EMS commits more reserve on average for all the tested uncertainty policies. On the other hand, the SO-based approach shows the highest levels of reserves for all methods which, and also yields higher total costs.

B. Computational Performance

Table III presents computational performance of the different study cases based on the number of iterations of the bi-level RUC formulation. It can be observed that, in most cases, the number of iterations ranges from 1 to 4; however, in cases of overly conservative policies (e.g., $\Gamma = 16$, $\Delta P_{\omega,t}^{max} = 37\%$), the algorithm does not converge within 10 iterations. This is due to the fact that, as the levels of conservatism increase, some uncertainty policies produce solutions of the sub-problem that have the same cost function value with different $\Delta P_{\omega,t}$ results in the RUC sub-problem, thus slowing down the convergence speed. It has been observed that after 10 iterations the test cases would not converge at all even for large iteration limit. This is due to the over-conservativeness of the uncertainty policies, which translates into too many possible worst-case scenarios for the cutting-plane algorithm, thus making over-conservative uncertainty policies impractical. It is important to note that, unless the conditions change drastically from one hour to the next, the algorithm will not be required to perform many iterations to obtain a new set of results.

The number of iterations required for the RUC to converge is also affected by the optimality criterion of the MILP solver and the convergence criterion of the primal cutting-plane. In this case, CPLEX defines the relative tolerance of the branch-and-bound solving algorithm for the gap between the best integer objective and the objective of the best remaining node [36]. If this tolerance is too high, such as the default of 10%, the primal cutting-plane algorithm is unable to converge in less than 10 iterations. For this reason, the gap criteria must be set very tight (e.g., `OPTION OPTCR=0.01`). On the other hand, the convergence tolerance for the cutting-plane algorithm is set at 0.1%, with the aim of testing the proposed model with

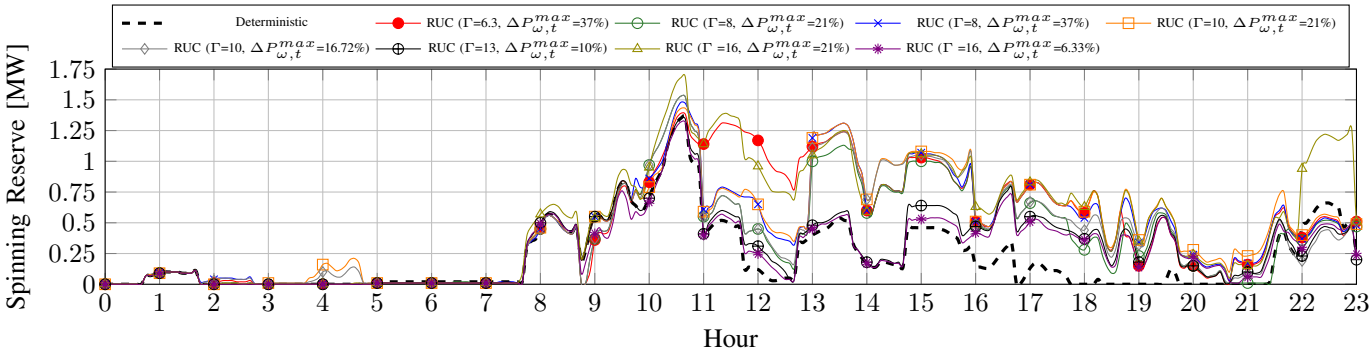

Fig. 8. Experiment 1 Spinning Reserve.

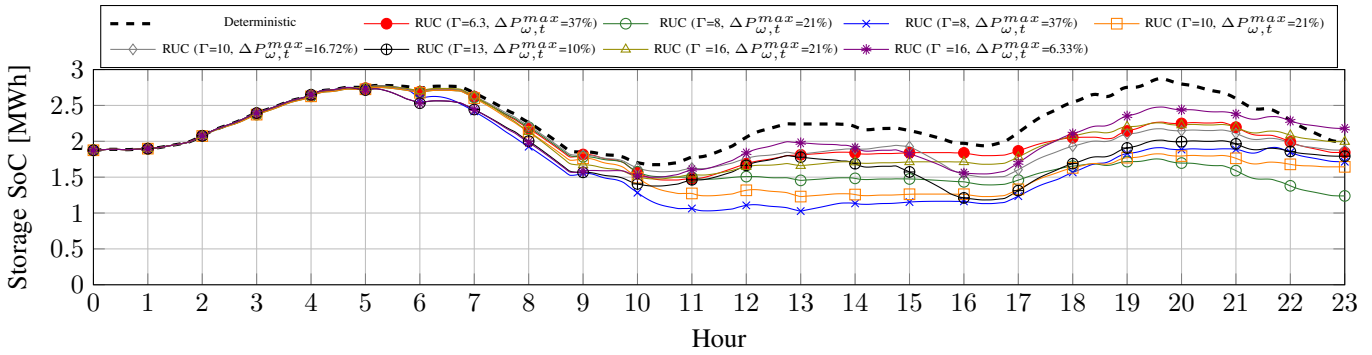

Fig. 9. Experiment 1 SoC of the ESS.

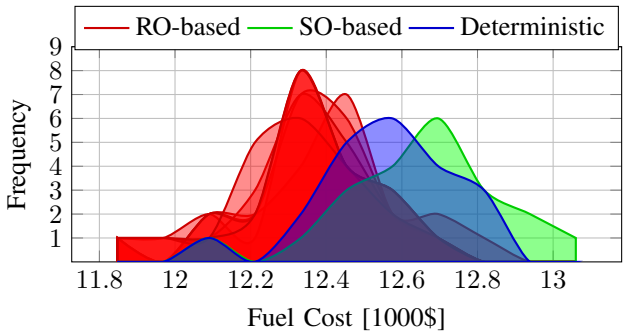

Fig. 10. Experiment 2 total fuel costs comparison.

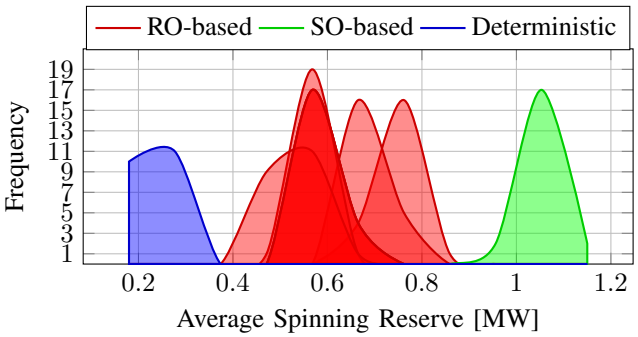

Fig. 12. Experiment 2 average reserve comparison.

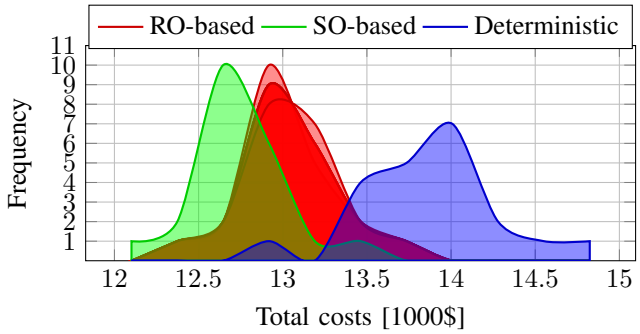

Fig. 11. Experiment 2 total costs comparison.

strict convergence criteria. Computational times averaged 6 s per OPF (NLP) calculation, and 60 s for the RUC; the larger share of processing time is to solve the sub-problem model. Solution times of the RUC were fairly constant for all the uncertainty policies, whereas solution times for OPF ranged from approximately 10 s for the 15 time-step windows, after an RUC update, to approximately 2 s for the shortest window right before the RUC update and window extension. Note that the solution times and implementation scheme are adequate for online applications. The EMS was tested on a fairly large isolated microgrid with a wide variety of DERs with results obtained in much less than the 5-minute window for the OPF and 1-hour window for the RUC.

C. Discussion

The results show that through a proper selection of the uncertainty policy $(\Gamma, \Delta P^{max}_{\omega,t})$, both a better economic per-

formance and more secure operation can be obtained with respect to the deterministic approach. The results in Table II show different economic performance of the EMS for different values of $\Delta P_{\omega,t}^{max}$ and Γ. These results reflect the importance of a proper selection of the uncertainty policy according to the specific characteristics of the forecasting system and the microgrid. In terms of the SoC levels, there are noticeable differences between the deterministic and robust case studies, since the robust formulation leads to a higher utilization of the ESS, and a flatter profile of SoC levels.

The results of the UC for different uncertainty policies show how the conservatism level changes depending on the value of $(\Gamma, \Delta P_{\omega,t}^{max})$; the reserves get higher and the SoC of the storage get reduced (see Figs. 8 and 9). In every case, the RUC consistently committed more units than the deterministic variant between hours 16-24, as a result of the high risk of mismatch in those hours, thus forcing the EMS to yield more reserves. Another relevant result can be observed at hours 11 to 13, where the RUC policies with large levels of Γ or $\Delta P_{\omega,t}^{max}$ commit an extra unit in order to charge the ESS; this difference is due to the interaction of the UC decisions with the management of the ESS SoC in the optimization algorithm.

The SoC levels reflect how much diesel spinning reserves the algorithm allocates to compensate for possible deviations in the RE. There are noticeable differences between the uncertainty policies since the robust formulation leads to a higher utilization of the ESS, as well as a flatter profile of SoC levels, as shown in Fig. 9. This is consistent with a more conservative management of the diesel resources. The results are consistent with the hours where the data shows high penetration of wind power, confirming the capability of the proposed approach to provide the system with extra resources during these critical hours.

Figure 6 shows the result of the worst-case scenario for a forecast issued for $t1$ (as depicted in Fig. 3), using the uncertainty policy that shows the best performance, i.e., for $\Gamma = 16$ and $\Delta P_{\omega,t}^{max} = 21\%$ and the respective uncertainty boundaries. The proposed algorithm determines that the worst mismatch is for the lower bound corresponding to the high penetration hours. This figure also depicts the realization of the wind power in a 5-minute timescale, showing the limitations of forecasting for isolated microgrids.

1) Effectiveness of the RUC approach: The simulations of the different net load scenarios in Experiment 2 show that the RO-based approach in the EMS is capable of producing satisfactory dispatch signals to hedge the system against forecasting errors. Moreover, in terms of total costs, it consistently outperforms the deterministic approach.

In terms of reserve levels, the RO-based approach allocates 0.6 MW of reserve on average, compared to the 0.22 MW of the deterministic case. Hence, the reserves levels were 13.84% percent of the peak load on average. The results from the simulations for the different uncertainty policies and wind power profiles demonstrate that an improved economic performance and a more secure operation can be obtained with the proposed RO-based EMS.

2) Comparison with SUC: The results of the top-performing uncertainty policy, i.e., $\Gamma = 16$, $\Delta P_{\omega,t}^{max} = 21\%$, when compared with respect to the scenario-based SO-based approach described in [20] for the 24-hour net load realization of Experiment 1, show that the SO-based approach resulted in a lower use of interruptible load as compared with the proposed RO-based approach, i.e., 44 kWh versus 175 kWh. Therefore, in general, the SO-based approach performs slightly better than the RO-based approach in terms of total costs, as shown in Experiment 2.

VI. Conclusions

This paper has presented a novel EMS algorithm for isolated microgrids with intermittent energy sources, combining the use of RHC formulations and recourse models based on a RO framework, in order to produce an economical and reliable microgrid dispatch without requiring probabilistic information from the forecast. The simulations results have demonstrated that through a proper selection of the uncertainty policy, improved performance and a more secure operation could be attained. It has been shown that the economic performance of the EMS for various uncertainty policies depends on the selection of the uncertainty policy. Overall, even though the fuel costs for the different RUC variants showed only marginal reduction, it has been shown that important improvements to the secure operation of the microgrid can be achieved by means of additional reserves and better management of the ESS. Furthermore, the RUC was able to produce hedged UC results without considering any probabilistic information from the forecasting system for on-line applications.

The main contributions of the research presented in this paper are:

- A novel and comprehensive EMS architecture and mathematical model that combines RHC and robust optimization in a two-stage recourse framework. The RUC model yields hedged commitment decisions according to an adjustable budget of uncertainty, whereas the final dispatch is calculated using a highly detailed three-phase OPF formulation. This proposed approach outperforms the deterministic approach in terms of reducing total operation costs, without requiring scenarios of forecast errors as other methods.
- Master- and sub-problem models to solve the RUC using a state-of-the-art primal cutting-planes algorithm which uses the SoC of the ESS in the recourse actions (a target value in the three-phase OPF) of the EMS to hedge against forecast uncertainty.
- A practical framework for the sizing of the uncertainty set based on the historical performance of the forecasting system. The presented tests show that the application of this approach provides the microgrid system operator with a simple and coherent procedure for calibrating the level of conservatism of the EMS.
- A thorough benchmarking analysis of the RO-based EMS that demonstrates the advantages of the proposed approach, producing the hedged UC results without any probabilistic assumptions about the forecasting system.

REFERENCES

[1] N. Hatziargyriou, H. Asano, R. Iravani, and C. Marnay, "Microgrids," *IEEE Power and Energy Magazine*, vol. 5, no. 4, pp. 78–94, 2007.

[2] D. Olivares, A. Mehrizi-Sani, A. Etemadi, C. Canizares, R. Iravani, M. Kazerani, A. Hajimiragha, O. Gomis-Bellmunt, R. Saeedifard, M. Palma-Behnke, A. Jimenez-Estevez, and N. Hatziargyriou, "Trends in microgrid control," *IEEE PES TF in Microgrid Control IEEE Trans. Smart Grid*, vol. 6, no. 4, pp. 1905–1919, July 2014.

[3] A. Parisio, E. Rikos, and L. Glielmo, "A model predictive control approach to microgrid operation optimization," *IEEE Trans. Control Systems Technology*, vol. 22, no. 5, pp. 1813–1827, Sept. 2014.

[4] L. Xie and M. Ilic, "Model predictive economic/environmental dispatch of power systems with intermittent resources," in *Power Energy Society General Meeting*, 2009, pp. 1–6.

[5] M. Korpas and A. Holen, "Operation planning of hydrogen storage connected to wind power operating in a power market," *IEEE Trans. Energy Conversion*, vol. 21, no. 3, pp. 742 –749, Sept. 2006.

[6] R. Palma-Behnke, C. Benavides, F. Lanas, B. Severino, L. Reyes, J. Llanos, and D. Saez, "A microgrid energy management system based on the rolling horizon strategy," *IEEE Trans. Smart Grid*, vol. 4, no. 2, pp. 996–1006, 2013.

[7] D. E. Olivares, C. A. Caizares, and M. Kazerani, "A centralized energy management system for isolated microgrids," *IEEE Trans. on Smart Grid*, vol. 5, no. 4, pp. 1864–1875, July 2014.

[8] B. Abegaz, S. M. Mahajan, and E. N. Olana, "Optimal energy management for a smart grid using resource-aware utility maximization," *International Journal of Emerging Electric Power Systems*, vol. 17, 01 2016.

[9] M. Marzband, F. Azarinejadian, M. Savaghebi, and J. M. Guerrero, "An optimal energy management system for islanded microgrids based on multiperiod artificial bee colony combined with markov chain," *IEEE Systems Journal*, vol. 11, no. 3, pp. 1712–1722, Sept 2017.

[10] Y. Zhang, N. Gatsis, V. Kekatos, and G. Giannakis, "Risk-aware management of distributed energy resources," in *18th Int. Conference on Digital Signal Processing*, July 2013, pp. 1–5.

[11] A. Hooshmand, M. Poursaeidi, J. Mohammadpour, H. Malki, and K. Grigoriads, "Stochastic model predictive control method for microgrid management," in *IEEE PES Innovative Smart Grid Technologies*, Jan. 2012, pp. 1–7.

[12] B. Zhao, Y. Shi, X. Dong, W. Luan, and J. Bornemann, "Short-term operation scheduling in renewable-powered microgrids: A duality-based approach," *IEEE Trans. Sustainable Energy*, vol. 5, no. 1, pp. 209–217, Jan. 2014.

[13] P. Pinson, "Wind energy: Forecasting challenges for its operational management," *Statistical Science*, pp. 564–585, 2013.

[14] W. Su, J. Wang, and J. Roh, "Stochastic energy scheduling in microgrids with intermittent renewable energy resources," *IEEE Trans. on Smart Grid*, vol. 5, no. 4, pp. 1876–1883, July 2014.

[15] Y. Zhang, N. Gatsis, and G. Giannakis, "Robust energy management for microgrids with high-penetration renewables," *IEEE Trans. Sustainable Energy*, vol. 4, no. 4, pp. 944–953, Oct 2013.

[16] M. Burger, G. Notarstefano, and F. Allgower, "A polyhedral approximation framework for convex and robust distributed optimization," *IEEE Trans. Automatic Control*, vol. 59, no. 2, pp. 384–395, Feb. 2014.

[17] A. Thatte, L. Xie, D. Viassolo, and S. Singh, "Risk measure based robust bidding strategy for arbitrage using a wind farm and energy storage," *IEEE Trans. Smart Grid*, vol. 4, no. 4, pp. 2191–2199, Dec. 2013.

[18] W. Wu, J. Chen, B. Zhang, and H. Sun, "A robust wind power optimization method for look-ahead power dispatch," *IEEE Trans. Sustainable Energy*, vol. 5, no. 2, pp. 507–515, April 2014.

[19] E. Kuznetsova, Y.-F. Li, C. Ruiz, and E. Zio, "An integrated framework of agent-based modelling and robust optimization for microgrid energy management," *Applied Energy*, vol. 129, pp. 70–88, 2014.

[20] D. E. Olivares, J. D. Lara, C. A. Caizares, and M. Kazerani, "Stochastic-predictive energy management system for isolated microgrids," *IEEE Trans. Smart Grid*, vol. 6, no. 6, pp. 2681–2693, Nov. 2015.

[21] S. Paudyal, C. Canizares, and K. Bhattacharya, "Optimal operation of distribution feeders in smart grids," *IEEE Trans. Industrial Electronics*, vol. 58, no. 10, pp. 4495–4503, 2011.

[22] A. Ben-Tal, A. Goryashko, E. Guslitzer, and A. Nemirovski, "Adjustable robust solutions of uncertain linear programs," *Mathematical Programming*, vol. 99, no. 2, pp. 351–376, 2004.

[23] M. Arriaga, C. Canizares, and M. Kazerani, "Renewable energy alternatives for remote communities in northern ontario, canada," *IEEE Trans. Sustainable Energy*, vol. 4, no. 3, pp. 661–670, July 2013.

[24] B. Zhao, X. Zhang, J. Chen, C. Wang, and L. Guo, "Operation optimization of standalone microgrids considering lifetime characteristics of battery energy storage system," *IEEE Trans. Sustainable Energy*, vol. 4, no. 4, pp. 934–943, Oct. 2013.

[25] A. Ben-Tal, D. Den Hertog, A. De Waegenaere, B. Melenberg, and G. Rennen, "Robust solutions of optimization problems affected by uncertain probabilities," *Management Science*, vol. 59, no. 2, pp. 341–357, 2013.

[26] D. Bertsimas, D. B. Brown, and C. Caramanis, "Theory and applications of robust optimization," *SIAM review*, vol. 53, no. 3, pp. 464–501, 2011.

[27] D. Bertsimas and M. Sim, "The price of robustness," *Operations Research*, vol. 52, no. 1, pp. 35–53, 2004.

[28] J. Morales, A. J. Conejo, P. Madsen, H. Pinson, and M. Zugno, *Integrating Renewables in Electricity Markets*, 1st ed., ser. Springer International Series in Operations Research & Management Science. Springer US, 2014, vol. 205.

[29] A. Nemirovski, "Lectures on robust convex optimization," Georgia Inst. of Technol., Tech. Rep., 2009.

[30] Z. Bo and Z. Long, "Solving two-stage robust optimization problems using a column-and-constraint generation method," *Operations Research Letters*, vol. 41, no. 5, pp. 457 – 461, 2013.

[31] L. Zhao and B. Zeng, "Robust unit commitment problem with demand response and wind energy," in *IEEE PES General Meeting*, July 2012, pp. 1–8.

[32] D. Bertsimas and J. N. Tsitsiklis, *Introduction to linear optimization*. Athena Scientific Belmont, MA, 1997.

[33] M. Zugno and A. J. Conejo, "A robust optimization approach to energy and reserve dispatch in electricity markets," Technical University of Denmark, Tech. Rep., 2013.

[34] S. A. Gabriel and F. U. Leuthold, "Solving discretely-constrained MPEC problems with applications in electric power markets," *Energy Economics*, vol. 32, no. 1, pp. 3 – 14, 2010.

[35] R. E. Rosenthal, *GAMS – A User's Guide*, GAMS Development Corporation, Washington, DC, USA, December 2012.

[36] CPLEX, IBM ILOG, "V12. 1: User's manual for cplex," *International Business Machines Corporation*, vol. 46, no. 53, p. 157, 2009.

[37] A. Wächter and L. T. Biegler, "On the implementation of an interior-point filter line-search algorithm for large-scale nonlinear programming," *Mathematical Programming*, vol. 106, pp. 25–57, 2006.

[38] CIGRE Task Force C6.04 and K. Strunz, "Benchmark systems for network integration of renewable and distributed energy resources," *CIGRE Technical Report*, May 2013.

[39] G. Papaefthymiou and B. Klockl, "Mcmc for wind power simulation," *IEEE Transactions on Energy Conversion*, vol. 23, no. 1, pp. 234–240, March 2008.

Jose D. Lara (S'11, M'15) was born in San José Costa Rica, received the B.Sc. and Licentiate in Electrical Engineering from the University of Costa Rica in 2009 and 2012 respectively, M.Sc. degree in Electrical and Computer Engineering from the University of Waterloo, Canada in 2014, and a M.S. in Energy and Resources from the University of California Berkeley in 2017, where is currently a PhD student at the Energy and Resources Group. His research interests include analysis and simulation of power systems, mathematical programming under uncertainty and its applications to power systems operation and quantitative energy policy.

Daniel E. Olivares (S'11, M'14) was born in Santiago, Chile, received the B.Sc. and the Engineer degree in electrical engineering from the University of Chile, Santiago, Chile, in 2006 and 2008 respectively, and the Ph.D. degree in Electrical and Computer Engineering from the University of Waterloo, Waterloo, ON, Canada, in 2014. He is currently an Assistant Professor at the Electrical Engineering Department of the Pontificia Uiversidad Católica de Chile, Santiago, Chile. His research interests include the modeling, simulation, control and optimization of power systems in the context of smart grids.

Claudio A. Cañizares (S'86, M'91, SM'00, F'07) is a Professor and the Hydro One Endowed Chair at the ECE Department of the University of Waterloo, where he has held different academic and leadership positions since 1993. His highly cited research activities focus on modeling, simulation, computation, stability, control, and optimization issues in power and energy systems in the context of competitive energy markets, smart grids, and microgrids. He is a Fellow of the IEEE, of the Royal Society of Canada, and of the Canadian Academy of Engineering, and is the recipient of the 2017 IEEE PES Outstanding Power Engineering Educator Award, the 2016 IEEE Canada Electric Power Medal, and of other various awards and recognitions from IEEE PES Technical Committees and Working Groups, in which he has held/holds several leadership positions.